Turbidity Investigation of the Sol–Gel Transition in Carrageenan Gels Under Physiologic Conditions

YUANYE CHEN,[1] ZHIBING HU,[1] JOHN C. LANG[2]

[1] Department of Physics, University of North Texas, Denton, Texas 76203

[2] Alcon Laboratories, Inc., Fort Worth, Texas 76134

Received 19 March 1997; accepted 27 August 1997

ABSTRACT: A spectrophotometer was used to measure the turbidity of a carrageenan gel as a function of temperature. The optical transmission of the gels was found to decrease as the gels undergo the sol–gel phase transition. The differential of transmission (I) with respect to temperature (T), dI/dT, exhibits peaks for both the cooling and the heating runs with the peak positions corresponding to temperatures of gelation and melting, respectively. The full-width at half-height of the dI/dT peak obtained from the heating curve is about 2.5 times broader than that from the cooling curve. This indicates that the melting of gels may involve multiple relaxation mechanisms. The area of the hysteresis loop covered by the cooling and the heating curves increases with a decrease in the scanning rate. The thermal cycling has little impact on the sol–gel transition in the gels. The experiments show that turbidity is a powerful tool for studying the sol–gel transition in carrageenan gels. © 1998 John Wiley & Sons, Inc. J Appl Polym Sci 68: 29–35, 1998

Key words: carrageenan gel; turbidity method; sol–gel transition; biopolymers

INTRODUCTION

Carrageenan gels have been used not only as stabilizers and texturizers in a wide variety of food products,[1] but also as immobilization materials for various types of living cells.[2] The formation of a thermoreversible gel on cooling is related to the coil-to-helix transition.[3–5] The sol–gel transition in carrageenan gels, especially in κ-carrageenan, has been studied intensively because many physical and chemical properties are influenced by this change of state.[1] To characterize the sol–gel transition, many methods have been used, including X-ray diffraction,[6] differential scanning calorimetry,[7,8] electron spin resonance,[8] nuclear magnetic resonance (NMR),[9,10] dynamic light scattering,[11] and optical rotation.[4–12] The kinetics of ion-induced gelation in carrageenan gels has been revealed using the turbidity technique.[13] In this article, a study of the turbidity of the sol–gel transition of the carrageenan *Eucheuma gelatinae* is reported.

The total scattered light I_s is the summation of the scattered light in all directions[14,15]:

$$I_s(t) = 2\pi \int_0^{\pi} I_s(q, t)\sin(\theta)\, d\theta \qquad (1)$$

where θ is the scattering angle; q, the scattering wave vector; and t, the time. Since $q(\theta) = (4\pi n/\lambda)\sin(\theta/2)$, one has

$$I_s(t) = \frac{8\pi}{q_{\pi}^2} \int_0^{q_{\pi}} I_s(q, t) q\, dq \qquad (2)$$

Correspondence to: Z. Hu.

Contract grant sponsor: Donors of the Petroleum Research Fund, Alcon Laboratories, Inc.

Journal of Applied Polymer Science, Vol. 68, 29–35 (1998)
 CCC 0021-8995/98/010029-07

where $q_\pi = 4\pi n/\lambda$ is the wave vector of the scattered light; λ, the wavelength; and n, the refractive index. The turbidity A is defined as the reduction in fractional light intensity per unit penetration length in the sample, $A = -(1/I)(\delta I/\delta x)$, with I the light intensity in the sample. For a small enough δx, no multiple scattering will occur in δx and $(-\delta I)$ is equal to I_s:

$$A = \frac{1}{\delta x}\left(\frac{I_s}{I}\right) \tag{3}$$

The turbidity, which could involve multiple scattering, is therefore directly related to the scattering function I_s which does not involve multiple scattering.[16]

The transmitted light intensity I_t and the incident intensity I_0 are related to the sample turbidity A and thickness L (assuming no absorption by chromophores):

$$\frac{I_t}{I_0} = e^{-AL} \tag{4}$$

Therefore, turbidity can be obtained from the ratio of the transmitted light intensity to the incident intensity, $A = -(1/L)\ln(I_t/I_0)$.

EXPERIMENTAL

The gel samples with two polymer network concentrations (0.8 and 1.2 wt %) were prepared using standard methods. The optical transmission of the gel samples was monitored by a spectrophotometer operating at the wavelength (λ) of 555 nm. The turbidity from a sample of known thickness can be computed from transmission using eq. (4). The temperature of the sample was controlled by an external water circulator. In addition to the temperature sensor in the circulator, a thermocouple was placed inside the sample cell for temperature measurement. The cell was sealed using a plastic film to prevent evaporation. The accuracy of the temperature measurements in this experiment was estimated to be ± 0.5°C.

The biopolymer investigated was a low-sulfated carrageenan known to gel on exposure to monovalent alkali metal ions.[2] The biopolymer is isolated from selected fractions of seaweed of the class *Rhodophyceae,* genus *Eucheuma,* and species *gelatinae.*[17] The species κ-carrageenan is known to gel on exposure to potassium ions; *Eucheuma g*. is known to possess lower charge density and to gel on exposure to sodium ions. The ionic composition of this study represents the level of exposure expected under physiological conditions.

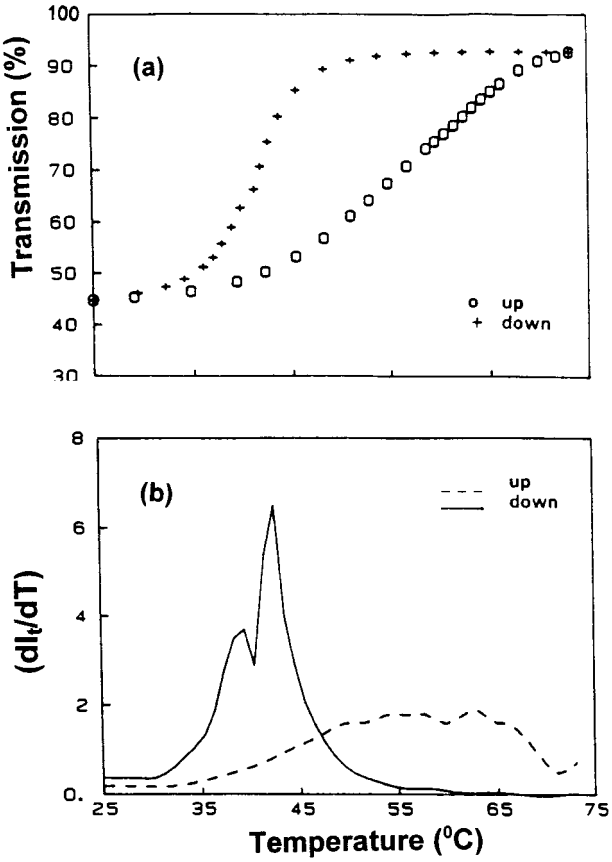

Figure 1 (a) Temperature dependence of turbidity for the 0.8% sample. The heating and cooling runs are represented by (○) and (+), respectively. The temperature scanning rates are 0.2°C/min for both runs. (b) The differential of the data curves (dI_t/dT) in (a). Solid and dashed lines represent the cooling and heating runs, respectively.

RESULTS AND DISCUSSION

The temperature dependence of the optical transmission ($I = I_t/I_0$) is plotted in Figure 1(a) for the 0.8% gel sample. The heating and cooling runs are represented by open circles and plus symbols, respectively. The scanning rate was 0.2°C/min for both runs. The sample was placed in a glass sam-

ple cell with dimensions of $1 \times 1 \times 5$ cm^3. Before measurement, the sample was melted and then cooled in the air to ambient temperature so that the sample in the glass cell was distributed uniformly. The sample was then heated from room temperature to 73°C and subsequently cooled to room temperature again. As the temperature was increased a second time, the transmission of the gels increased and finally reached a plateau at around $T = 73$°C. When the gel was cooled, the transmission of the gels decreased. Clearly, the transmission of the gel is associated with the gelation process. The more gel formed, the lower the optical transmission. This may be because the helix domains in the gelled state have spatial variations and dynamic concentration fluctuations which result in strong light scattering.[11,18]

The derivative of optical transmission with respect to temperature (dI_t/dT) is shown in Figure 1(b) for the 0.8% sample. The dI_t/dT curves exhibit peaks for both cooling (solid line) and heating (dashed line) runs with the peak positions corresponding to gelation (T_g) and melting temperature (T_m), respectively. The value of T_m is higher that of T_g, in agreement with previous optical rotation[4] and DSC results on κ-carrageenan.[7] The hysteresis loop has been interpreted in terms of stabilization of the ordered conformation by aggregation.[3] Furthermore, it is found that the change of transmission for the heating run is much slower than that for the cooling run near the phase transition. The full-width at half-height of the dI/dT curve obtained from the heating curve is 2.5 times broader than that from the cooling curve. It is known that the gelation process involves the transformation of carrageenan molecules from a coil-to-helical conformation and the subsequent helix aggregation. Both the formation of the helices and helix aggregation occur in a narrow temperature range, resulting in a sharp dI/dT peak. On the other hand, melting a helical structure occurs in a broad temperature range. This may be due to the interactions among helical structures having a broad distribution. Often, such hysteresis can result from thermodynamic constraints; for example, on cooling, if the system were to enter the spinodal region, a more abrupt transition would be observed. These phenomena are worth further investigation.

Figure 2(a,b) show the temperature dependence of the optical transmission and its differential with respect to temperature for the sample containing 1.2% polymer. The experimental conditions for the measurement are the same as those for the 0.8% sample. Neither melting temperature, T_m, nor gelation temperature, T_g, showed a significant shift when the polymer concentration was increased from 0.8 to 1.2%. The values of the transmission in the 0.8% sample are higher than those in the 1.2% sample at any given temperature. This indicates that density fluctuation in the 1.2% sample is greater than that in the 0.8% sample, as expected.

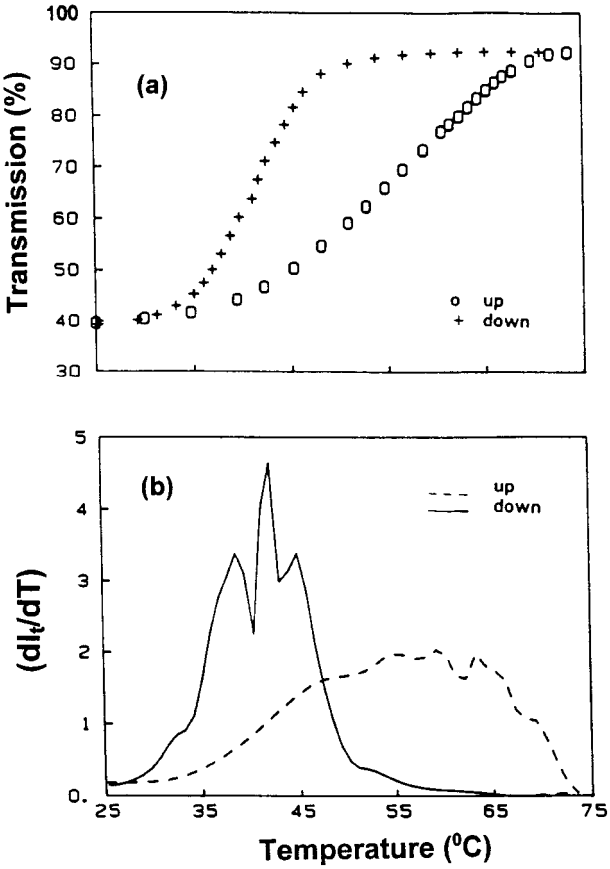

Figure 2 (a) Temperature dependence of transmission for the 1.2% sample. The heating and cooling runs are represented by (○) and (+), respectively. The temperature scanning rates are 0.2°C/min for both runs. (b) The differential of the data curves (dI_t/dT) in (a). Solid and dashed lines represent the cooling and heating runs, respectively.

It is to be noted that the temperature-dependent sol–gel transition is conventionally studied using differential scanning calorimetry (DSC).[7] The exothermic peak in the cooling DSC curve and the endothermic peak in the heating DSC curve were observed at T_g and T_m, respectively.

The intensity of the peaks increases with the scanning rate. At a very slow scanning rate, the peaks cannot be easily identified. For the turbidity measurement, the scanning rate can be as slow as possible. Therefore, the data may be used for testing both the thermodynamic models and kinetic models which are usually proposed for the thermal equilibrium systems.

The thermal cycling effect on the 0.8% sample is shown in Figures 3(a–c). The sample was first placed in the sample cell. Then, the optical transmission was measured as the sample was heated in the scanning rate of 0.2°C/min. When the sample reaches 73°C, it was cooled to room temperature as shown in Figure 3(a). The second and the third cycles are shown in Figure 3(b,c), respectively. Except for the first cycle where the transmission change around the T_m is sharper, the optical transmissions measured in thermal cycles are almost identical. Similar thermal cycling results were also obtained for the 1.2% sample as shown in Figures 4(a–c).

Figures 5(a–c) show the transmission in the 1.2% gel as a function of temperature at various scanning rates of (a) 0.1, (b) 0.2, and (c) 1°C/min. In these experiments, the samples were initially kept at 73°C for about 15 min so that they were completely melted. The samples were then cooled at a designated scanning rate. After the samples reached room temperature, they were heated to 73°C using the same scanning rate. It is clear from Figure 5 that the area of the hysteresis loop decreases as the scanning rate increases. This indicates that the gelation and melting processes do not have enough time to complete at a higher scanning rate. Furthermore, it is found that the transmission value in the gel at room temperature depends on the cooling rate. The higher the cooling rate, the higher the transmission value.

The transmission data in Figure 5 for different scanning rates were normalized by the expression

$$F(T) = \frac{I(T) - I_{\min}}{I_{\max} - I_{\min}} \qquad (5)$$

where $F(T)$ is the normalized transmission, and $I_{\min}$ and $I_{\max}$, the minimum and the maximum values of the transmission, respectively. The results are shown in Figure 6. It is apparent that

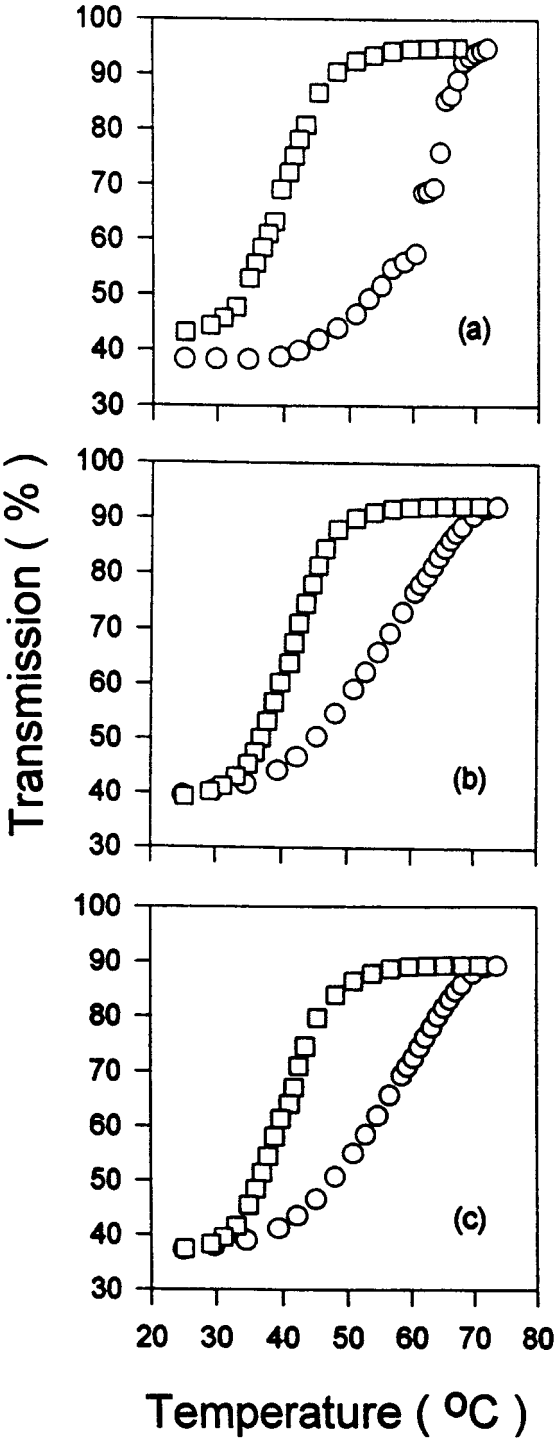

Figure 3 Thermal effect on the transmission versus temperature for the 0.8% sample. The thermal cycle starts at 73°C. The sample was first cooled and then heated to 73°C again. The scanning rate is 0.2°C/min. (a–c) represent the first, second, and third cycles, respectively.

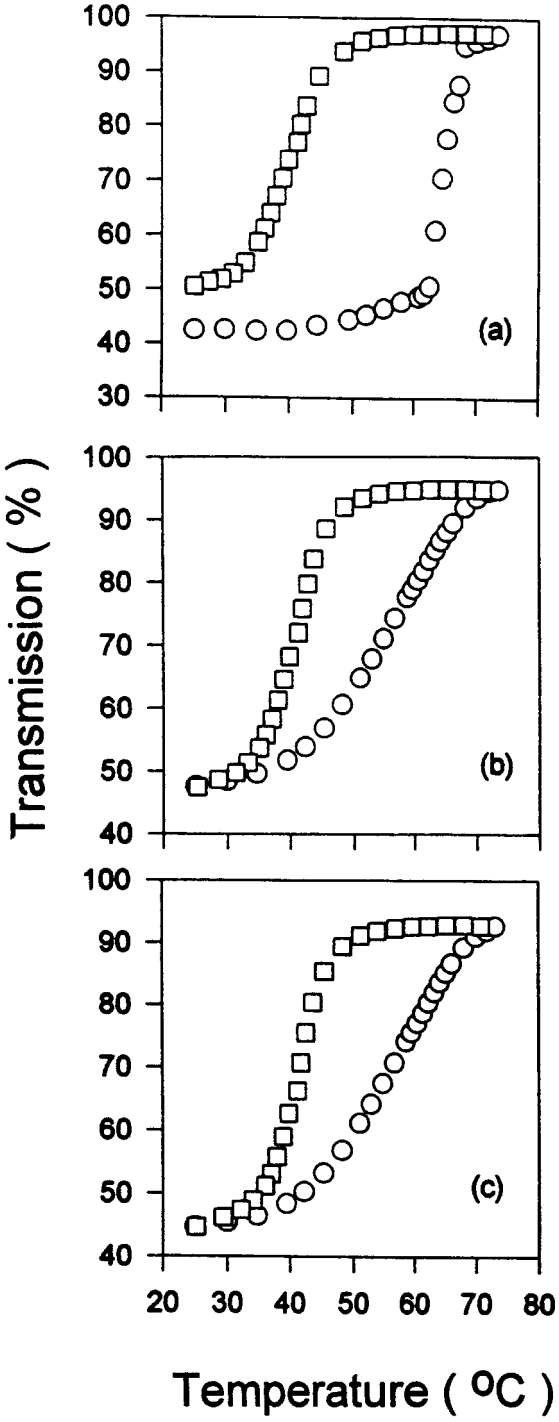

Figure 4 Thermal effect on the transmission versus temperature for the 1.2% sample. The thermal cycle starts at 73°C. The sample was first cooled and then heated to 73°C again. The scanning rate is 0.2°C/min. (a–c) represent the first, second, and third cycles, respectively.

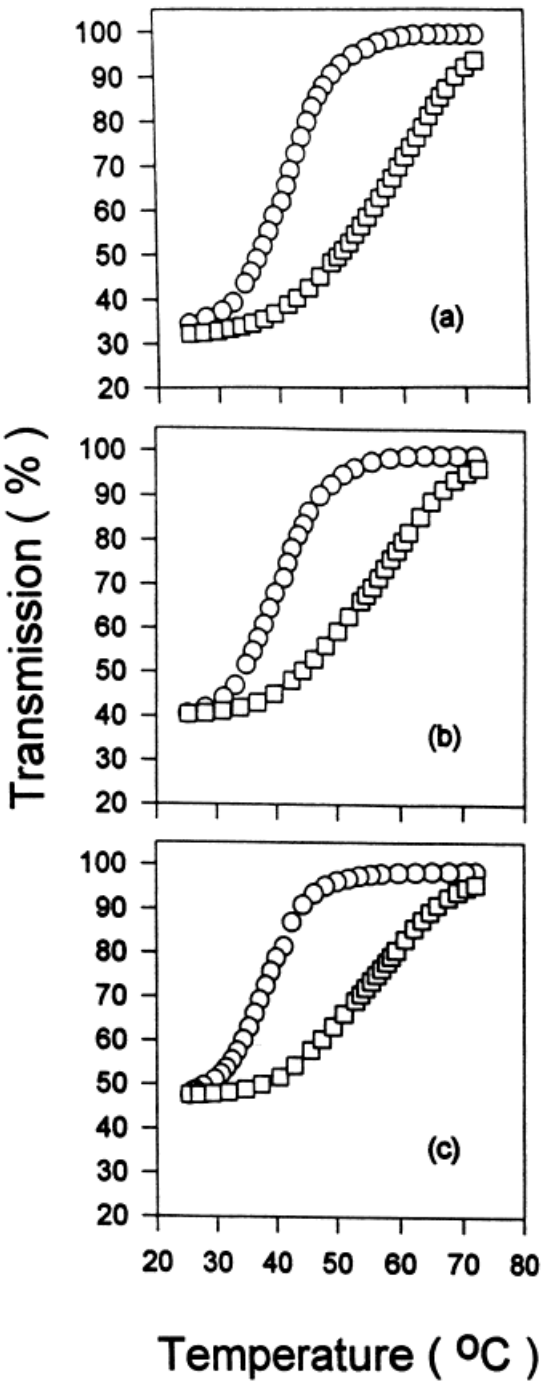

Figure 5 Transmission versus temperature for the 1.2% gel at various temperature scanning rates: (a) 0.1, (b) 0.2, and (c) 1°C min.

the hysteresis loop persists, even at a very slow scanning rate, indicating that the sol–gel transition in the gels is the first-order phase transition.

Defining T_{mid} as the temperature at which the normalized transmission data curves reach 50%, T_{mid} is slightly shifted to a lower temperature as the scanning rate is decreased as shown in Figure 7.

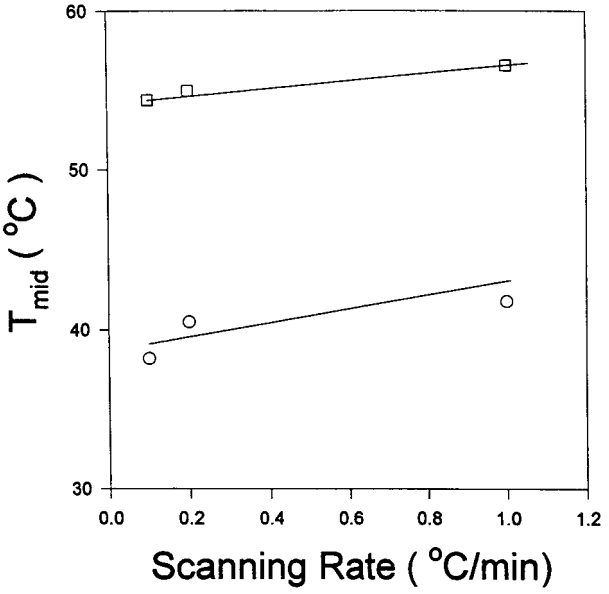

Figure 7 Scanning rate dependence of T_{mid} at which the normalized transmission data curves reach 50%. The cooling and the heating runs are represented by (○) and (□), respectively.

CONCLUSION

The optical transmission in carrageenan gels was measured successfully as a function of temperature. The melting point is found always to be higher than the gelation temperature. The area of the hysteresis loop decreases as the scanning rate increases. The thermal cycling has little impact on the sol–gel transition in the gels. The transmission value at room temperature is cooling-rate-dependent. The method applied here appears to offer a new, precise, and easy means to study both the sol–gel transition in carrageenan (and related) gels and related transitional properties, especially the kinetics of the process. This study demonstrates the potential of turbidity for studying the microstructure and dynamics.

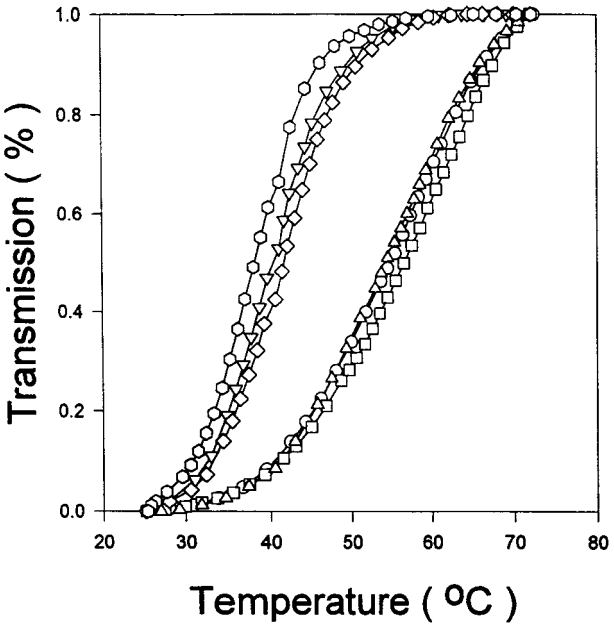

Figure 6 Normalized transmission versus temperature for various scanning rates: (△) up and (⬡) down (0.1°C/min); (○) up and (▽) down (0.2°C/min); (□) up and (◇) down (1°C/min).

Acknowledgment is made to the Donors of the Petroleum Research Fund, administered by the American Chemical Society, and Alcon Laboratories, Inc., for support of this research.

REFERENCES

1. N. F. Stanley, in *Food Gels,* P. Harris, Ed., Elsevier Science Publishers Lmt., New York), 1990, p. 79.
2. B. Mattiason, in *Immobilized Cells and Organelles, Vol. 1,* CRC Press, Boca Raton, FL, 1983, p. 3.
3. I. T. Norton, D. M. Goodall, E. R. Morris, and D. A. Rees, *Chem. Commun.,* 515 (1978).
4. E. R. Morris, D. A. Rees, and G. Robinson, *J. Mol. Biol.,* **138,** 349 (1980).
5. C. Rochas and M. Rinaudo, *Biopolymers,* **24,** 735 (1984).
6. D. A. Rees, *Biochem. J.,* **126,** 257 (1972).
7. K. Nishinari and M. Watase, *Thermochim. Acta,* **206,** 149 (1992).
8. P. A. Williams, S. M. Clegg, M. J. Langdon, K. Nis-

hinar, and L. Piculell, *Macromolecules,* **26,** 5441 (1993).
9. M. Tokita, K. Terakawa, T. Ikeda, and K. Hikichi, *Polym. Commun.,* **31,** 38 (1990).
10. W. Zhang and I. Furo, *Biopolymers,* **33,** 1714 (1993).
11. D. Slootmaekers, M. Mandel, and H. Reynaers, *Int. J. Biol. Macromol.,* **13,** 17 (1991).
12. C. Rochas, M. Rinaudo, and S. Landry, *Carbohydr. Polym.,* **12,** 255 (1990).
13. Z. Hu, Y. Chen, and J. C. Lang, *J. Appl. Polym. Sci.,* **60,** 221 (1996).
14. B. Chu, *Laser Light Scattering,* Academic Press, New York, 1974.
15. M. H. G. M. Penders and A. Vrij, *J. Chem. Phys.,* **93,** 3704 (1990).
16. Y. Li, G. Wang, and Z. Hu, *Macromolecules,* **28,** 4194 (1995).
17. Available from Marine Colloids Division of FMC.
18. R. Nossal, *Macromolecules,* **18,** 49 (1985).